frontiers | Frontiers in Environmental Science

TYPE Review
PUBLISHED 10 April 2023
DOI 10.3389/fenvs.2023.1093095

OPEN ACCESS

EDITED BY
Cheng Chen,
University of Lille, France

REVIEWED BY
Xuguang Tang,
Southwest University, China
Ruiwu Zhou,
Yuxi Normal University, China

*CORRESPONDENCE
Xuehai Fei,
feixuehai@gzu.edu.cn

SPECIALTY SECTION
This article was submitted to Environmental Informatics and Remote Sensing, a section of the journal Frontiers in Environmental Science

RECEIVED 08 November 2022
ACCEPTED 28 March 2023
PUBLISHED 10 April 2023

CITATION
Liao Z, Zhou B, Zhu J, Jia H and Fei X (2023), A critical review of methods, principles and progress for estimating the gross primary productivity of terrestrial ecosystems.
Front. Environ. Sci. 11:1093095.
doi: 10.3389/fenvs.2023.1093095

A critical review of methods, principles and progress for estimating the gross primary productivity of terrestrial ecosystems

Zhangze Liao[1,2,3], Binghuang Zhou[1,2,3], Jingyu Zhu[1,2,3], Hongyu Jia[1,2,3] and Xuehai Fei[1,2,3]*

[1]College of Resources and Environmental Engineering, Guizhou University, Guiyang, Guizhou, China, [2]Guizhou Karst Environmental Ecosystems Observation and Research Station, Ministry of Education, Guiyang, Guizhou, China, [3]Key Laboratory of Karst Geological Resources and Environment, Ministry of Education, Guiyang, Guizhou, China

The gross primary productivity (GPP) of terrestrial ecosystems reflects the total amount of organic carbon assimilated by vegetation through photosynthesis per given unit of time and area, which represents the largest carbon flux in carbon budget and plays a fundamental part in the carbon cycle. However, challenges such as determining how to select appropriate methods to improve GPP estimation accuracy at the regional/global scale remain. Therefore, it is of great importance to comprehensively review the research progress on the methods for estimating the GPP of terrestrial ecosystems and to summarize their flaws, merits and application fields. In this study, we reviewed studies of GPP estimation at different spatiotemporal scales, and systematically reviewed the principles, formulas, representative methods (Ground observations, Model simulations, SIF based GPP, and NIRv based GPP) at different scales and models (Statistical/Ecological process/Machine learning/Light use efficiency models), as well as the advantages and limitations of each research method/models. A comprehensive comparison of GPP research methods was performed. We expect that this work will provide some straightforward references for researchers to further understand and to choose appropriate models for assessing forest ecosystem GPP according to the research objectives and area. Thus, critical and effective GPP estimation methods can be established for the terrestrial carbon cycle, carbon neutralization accounting and local carbon emission reduction policy formulation and implementation.

KEYWORDS

ground observation-based GPP, model-based GPP, light use efficiency model, sun-induced chlorophyll fluorescence, near-infrared reflectance of vegetation

1 Introduction

The gross primary productivity (GPP) is the sum of gross carbon fixation by autotrophic carbon-fixing tissues per unit area and time (gross photosynthesis minus photorespiration) (Chapin et al., 2006; Wohlfahrt and Gu, 2015). GPP represents the material and energy that initially enters a terrestrial ecosystem and directly reflects the productivity of the terrestrial ecosystem under natural conditions (Yuan et al., 2014a). GPP is an important link

representing the capacity of vegetation fixing CO_2 in the carbon cycle through photosynthesis, drives seasonal and interannual changes in CO_2 contents and is also a key parameter for understanding atmosphere-biosphere interactions and the global carbon cycle (Christian et al., 2010; Yuan et al., 2014a).

The terrestrial ecosystem, as the most complex major carbon pool among the "four carbon pools" in the world (i.e., namely, the terrestrial ecosystem carbon pool, the lithosphere carbon pool, the ocean carbon pool and the atmospheric carbon pool) stores 25%–30% of anthropogenic CO_2 emissions (Qiu, 2015; Wang et al., 2017). This ecosystem type plays a vital role in maintaining the global carbon cycle and mitigating climate change (Cramer et al., 2001), and accurate quantification of GPP and its dynamic spatiotemporal changes is not only an important prerequisite for ecosystem function assessment and carbon balance research but can also serve as an important indicator for evaluating the support capacities of terrestrial ecosystems with regard to the sustainable development of human society (Yuan et al., 2014a; Tang et al., 2015). However, it is difficult to realize direct observations of GPP (Ma et al., 2015; Rahman et al., 2015). Conclusions based on ground observations, scattered spatial sampling and flux-site observations are applicable only within a limited spatial range. Similarly, data-driven and remote sensing model simulations make it possible to conduct quantitative research and obtain spatio-temporal dynamic of large-scale ecosystem GPP. Unfortunately, whether ground observations or model simulation research is conducted, GPP estimation results are always affected by environmental factors, model structures and the response modes of different vegetation types, which means great uncertainties exist in estimation results derived at different temporal and spatial scales. In addition, under the background of global climate change and the goals of "carbon peaking and carbon neutrality", increasing accuracy of regional/global GPP estimations is an important scientific and social need in the context of clarifying the current situation and establish the potential for regional carbon sequestration.

Therefore, in this paper, we review the progress of GPP research, systematically summarize the advantages and disadvantages of ground-observation and model-simulation methods, aim to systematically sort GPP estimation methods designed for different scales and their application potentials, comprehensively compare the characteristics of various models, and summarize the existing problems and possible development directions. We expect that this work will provide a reference for improving the quantitative GPP research methods and model-selection process. Thus, effective research methods for estimating the total amount of carbon sequestration in the regional carbon cycle, performing carbon neutralization accounting and formulating and implementing local carbon emission reduction policies are provided.

2 Research progress on GPP estimation methods

Since the launch of the International Biological Programme (IBP) in the 1960s, research on the GPP of terrestrial ecosystems has developed rapidly and has gone through stages such as field investigations, fixed-point observations and model simulations (Chen, 2017). In general, research on terrestrial ecosystem GPP estimation can be roughly divided into two aspects: ground observations and model simulations (Huang, 2019).

2.1 Ground observations

Ground observation research methods based on sample plots or stations continue to develop and improve, from the traditional biomass survey method to the chlorophyll determination method, radioactive labelling method, eddy covariance method, etc. In addition, ground observations accurately and rapidly record climate data characterizing continuous changes in light, temperature and water conditions in the analysed ecosystem, allowing a large number of reliable driving and verification data to be accumulated for subsequent GPP model simulations. At present, commonly used ecosystem-scale GPP ground observation methods include the biomass survey method and eddy covariance method.

2.1.1 Biomass survey methods

Biomass survey methods represent a traditional ecosystem productivity research method. Continuous biomass observations are the most basic means used to understand biomass accumulation dynamics, the relationships between ecosystem productivity and climate conditions, soil conditions and other factors, and the distributions of community photosynthetic products both aboveground and belowground. Biomass survey methods are simple and direct, but it is usually necessary to study continuous multiyears monitoring data to effectively reflect vegetation changes. Under certain conditions, GPP can be estimated using the dynamic monitoring data associated with ecosystem biomass change: this type ofchanges is formulated as GPP = NEP + R_a + R_h = NEP + R_{eco} (with net ecosystem production (NEP), ecosystem respiration (R_{eco}), autotrophic respriation (R_a), heterotrophic respriation (R_h)). Biomass survey methods are small-scale observation methods, that are easy to implement with simple tools, equipment and calculation methods. However, scale mismatch may occur if large-scale extrapolation is need when estimating regional GPP. Moreover, if we want to extrapolate biomass to GPP, we must determine some variables that are difficult to measure, such as root turnover. Therefore, the estimation accuracy of this method needs to be verified. Zhang et al. (2019) analysed and summarized regional and global biomass datasets and found serious inconsistencies in the aboveground forest biomass data; in addition, the estimation results obtained using these datasets were highly uncertain (Liang et al., 2020). Therefore, spatiotemporal GPP distribution estimations obtained with biomass survey methods can be quite different. At the same time, biomass survey methods lack the integration of information regarding the carbon flux process or relevant environmental variables in the corresponding time period, so the results obtained using these methods cannot reflect the carbon cycle process, the driving forces of the analysed ecosystem or the local feedback adjustment mechanisms. Thus, the estimation accuracy of these methods must be improved (Fei, 2018). This is mainly due to the differences in the structure and function of the ecosystems, resulting in significant differences in the data obtained. Due to the above limitations of traditional field measurements to estimate

biomass at a regional scale, remote sensing has been widely used for estimation in past decades due to its wide-area coverage capability. In remote sensing-based biomass estimation, field measurements remain important, especially because they are indispensable to both the calibration of remotely sensed data and the validation of estimated biomass results. To estimate the primary productivity of terrestrial ecosystems accurately at a regional scale, much effort is currently being focused on integrating field data with remotely sensed data such as optical, synthetic aperture radar (SAR) and light detection and ranging (LiDAR) data using advanced methods (Lim, 2003; Powell Scott et al., 2009; Sinha et al., 2015).

2.1.2 Eddy covariance methods

At the ecosystem scale, eddy covariance (EC) methods can be used to obtain GPP ground observations by measuring the net ecosystem exchange (NEE) between the biosphere and the atmosphere and calculating the GPP of the vegetation (GPP = –NEE + R_{eco}). Specifically, at night, when vegetation does not carry out photosynthesis, the GPP is zero, and the NEE and R_{eco} are equal. According to the observed NEE data collected at night, the R_{eco} estimation equation can be established, and the daytime R_{eco} can be estimated in combination with the daytime NEE to further calculate GPP (Christian et al., 2010). This method has become the most important method for measuring CO_2 exchanges between vegetation and the atmosphere and is also an internationally recognized standard method for measuring carbon fluxes (Schimel et al., 2015). In the 1990s, an international geosphere-biosphere programme with global climate change research as the core was formed to directly promote and accelerate the construction and development of the global flux observation network (FLUXNET), and a carbon flux observation network system covering different climatic zones and typical vegetation ecological areas around the world was gradually established. To date, carbon flux networks that include more than 900 flux observation stations have been formed; for example, in Asian flux network and the China flux observation and research alliance provide long-term continuous carbon-flux observation data collected at multiple time scales (Friend Andrew et al., 2007) and covering almost all representative ecosystem types (Yuan et al., 2014a). China formally established a national carbon flux observation network in 2002. After more than 20 years of development, nearly 100 flux observation sites and research stations have been built nationwide (details can be found at http://www.chinaflux.org/general/index.aspx?nodeid=12). The continuous observation of CO_2 fluxes in various ecosystems, such as forests, grasslands, wetlands, farmlands, deserts, cities and water areas, has been realized (Yu et al., 2016). At the ecosystem scale, EC methods can provide direct observations at a high precision (measurable trace (<0.005 mg C m^{-2} s^{-1}) turbulent flux), high temporal resolution (the data output recording frequency is 10 or 20 Hz) and over a wide range. In addition, these methods have a solid theoretical foundation with regard to the observation and accounting processes. However, these field-based flux observations are affected by topography and geomorphology, and this method is applicable only to areas with relatively flat underlying surfaces and uniform canopy structures. At the same time, the actual data-sampling areas monitored by eddy covariance methods are limited to a small footprint (~1 km). The GPP values estimated using this method thus represent the entire studied ecosystem, exhibiting high temporal heterogeneities and a very limited spatial representation. In addition, large amounts of funds and labour are required for the construction and, later, maintenance of flux towers, so the current number of stations is sparse and very limited, making it difficult to obtain spatial or temporal GPP patterns on the regional or global scale (Zhao et al., 2019). Nevertheless, when we explore the coupled carbon-nitrogen-water cycles of forest ecosystems and their biological regulation mechanisms and analys the response and adaptation mechanism of forest ecosystem carbon cycle processes under the background of global change (Zhu et al., 2021), the data obtained using EC methods still play an irreplaceable role in carbon cycle research and in verifying the estimation accuracies of GPP models (Zhang, 2020).

2.2 Model simulations

The key problem restricting GPP simulations in regional/global terrestrial ecosystems is the lack of reliable, large-scale validation data, and this lack of data has greatly limited model development for a long time. Therefore, obtaining accurate, rapid, continuous and extensive ground observations has become a key way to solve this problem (Yuan et al., 2014a). Since the 1990s, with the increasing popularity of a variety of medium and high-resolution satellite data and the accumulation of eddy covariance flux data worldwide, many GPP estimation models have been developed. These models can be roughly divided into statistical models, ecological process models, light use efficiency (LUE) models and machine learning methods (Lin et al., 2018; Zhu, 2021). At the regional and even global scales, estimating GPP with LUE models based on remote sensing data has become an important and widely accepted research method (Chen et al., 2014; Shi, 2019). The uncertainty in remote sensing data products and the resulting C flux estimates can limits or comparisons of the magnitude, interannual variability, and long-term trends in vegetation productivity. As mentioned earlier, satellite-derived VIs are widely used as proxies of GPP, while LUE models, machine learning approaches, and diagnostic process-based models are routinely used to quantify GPP (Xiao et al., 2019).

2.2.1 Statistical models

Statistical models, also known as climate productivity models, are used to estimate vegetation productivity by establishing mathematical models through several common statistical methods according to the relationships between plant biomass changes and climate factors. For example, the Miami model (Helmut, 1975), Thornthwaite model (Wickens et al., 1977) and Chikugo model (Uchijima and Seino, 1985) have been widely used in regional GPP estimations. The model simulation process is shown in Figure 1. However, the Miami model considers only two limiting factors, temperature and precipitation, and this model feature has some defects. Based on the Miami model, the Thornthwaite model increases the impact of evapotranspiration on plant photosynthesis and improves the resulting estimation accuracy. Furthermore, considering that the absorption of photosynthetically effective

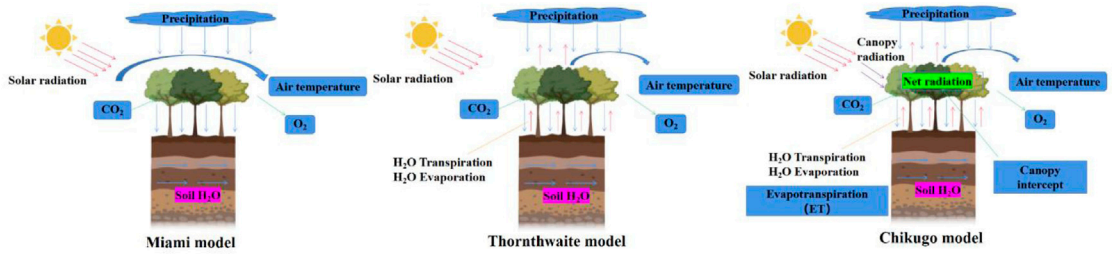

FIGURE 1
Schematic simulation process of typical statistical models.

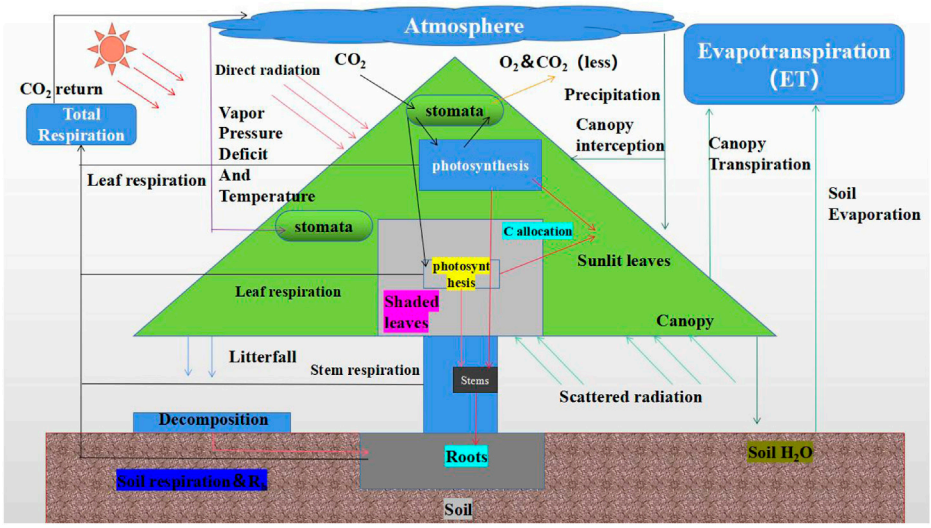

FIGURE 2
Process and mechanism of ecological process model.

radiation by vegetation canopies is one of the leading factors affecting photosynthesis, the Chikugo model adds the radiation dryness index and net radiation to calculate vegetation productivity, providing a more accurate description of productivity. Chen (1987) used the improved Miami model to calculate GPP in China, drew an online map and concluded that the distribution trend of biomass in China gradually decreased from southeast to northwest. This kind of model also has the advantages of simple model structures, few parameters and easy data acquisition. Correspondingly, the impact factors (temperature and precipitation) considered in the models are excessively simple, the complex ecosystem process is simplified, the physiological basis is not sufficiently strict, and the estimation results are uncertain. Specifically, when applied in arid and semiarid grassland areas, the values estimated by these models are high (Wen et al., 2014). At the same time, in areas with high productivity, the productivity continues to increase while the vegetation index becomes saturated. The correlation between these two factors gradually decreases, failing to reflect the response of the carbon sequestration process to climate change. In addition, these models lack a rational description of the vegetation productivity formation process (Yuan et al., 2014a). Therefore, they cannot be used for future prediction research but can be used only to assess real productivity.

2.2.2 Ecological process models

Ecological process models, also known as mechanism models, are depict the physiological and ecological mechanisms associated with vegetation growth and development in detail, such as radiative transfer, photosynthesis, respiration, evapotranspiration, and soil processes (Hall et al., 2012; Zhang et al., 2021). Thus, these models are built to estimate the GPP of terrestrial ecosystems. Such models include the Biome Bio-Geochemical Cycles (BIOME-BGC) model (Running Steven, 1993), Boreal Ecosystem Productivity Simulator (BEPS) model (Running Steven and Joseph, 1998), Lund-Postdam-Jena (LPJ) model (Sitch et al., 2003), and Century model (Huang, 2000). This kind of model provides a solid theoretical foundation and can clearly simulate the ecological mechanisms of plants. These models usually regard the vegetation canopy as big leaf/two leaf when computing ecosystem GPP. The main steps in the ecological

process model is shown in Figure 2. The main principles of the corrcsponding models are described below.

a) Big-leaf (BL) models regard the whole canopy as an extended leaf, thus extending the leaf-level model type to the canopy scale and achieving estimating GPP at the canopy scale. Representative BL models include the Simple Biosphere (SIB2) (Sellers et al., 1996), Biome-BGC and CLASS models (Wang et al., 2001). These BL models simplify the canopy structure and continuously improve the mechanism simulation effect. A canopy photosynthetic model can be expressed as follows:

$$P = P(R_{cc}) \quad R_{cc} = R_{sc}/LAI \qquad (2-1)$$

where $P(R_{CC})$ represents the canopy photosynthesis function, R_{CC} is the canopy conductance, R_{SC} is the leaf stomatal conductance, and LAI is the leaf area index. However, leaf photosynthesis exhibits a non-linear response to stomatal conductance which leads to large deviations between the calculated results and the actual values (Feng et al., 2004). In addition, the photosynthetic rates of leaves differ between direct radiation and scattered radiation conditions. Leaves under direct radiation are limited by temperature and nutrients, while leaves under scattered radiation are mainly limited by solar radiation. In addition, in BL models, the differences between shaded leaves and sunlit leaves are ignored.

b) Based on BL models, two-leaf (TL) models calculate the photosynthetic rates of two leave types according to the transport models of negative and positive leaves and finally superimpose these two photosynthesis values to obtain the canopy GPP. Typical TL models include the BEPS model, Community Land Model (CLM) and Dynamic Land Ecosystem Model (DLEM) (Liu et al., 1997; Tian et al., 2010; Chen et al., 2012). In addition, multilayer models divide the vegetation canopy (including leaves and air) into several vertical layers, calculate the flux layer-by-layer, and finally accumulate these fluxes to the canopy scale. Multilayer models, including the spatial production allocation model (SPAM) and CANWHT model (Feng et al., 2004), also distinguish between shaded leaves and sunlit leaves. The estimation results of such models are more accurate than those of simpler models, but these multilayer models require more parameters and are relatively complex.

Ecological process models exist in many forms have complex structures, require many input parameters and are difficult to obtain. Although significant progress has been made in the development of ecological process models over the past few decades, there are still many areas that need to be improved with regard to the GPP simulation performances of these models. The GPP simulation results estimated by these models are highly sensitive to the input parameters, and these models are applicable only to typical areas containing a single vegetation type or spatial scale. It is difficult to find models that are suitable for specific research areas or research directions with practical applications. In addition, the availability and accuracy of the required data cannot be guaranteed during the practical application process, and great uncertainties arise in the simulation results. Therefore, this kind of model is difficult to extend to regional-scale applications, and the advantages of the model mechanisms cannot be effectively brought into play.

2.2.3 Machine learning methods

Ecological process models have a sound scientific basis but rely on climate forcing variables and model parameterization (Zhang et al., 2021). These uncertainties lead to differences in the simulation results. Machine learning models are data-driven models based on mathematical and statistical principles and establish the non-linear relationships between input and target features by minimizing the loss function mostly through an iterative training process. These methods summarize the relationships between the carbon cycle and observation variables from a statistical point of view with data-driven techniques. In addition, machine learning methods can limit the uncertainties associated the parameterization scheme, model structure and input variables of traditional empirical and ecological process models when simulating GPP. With the development of computer science, increasing attention has been paid to research on GPP inversion simulation methods that involve the use of remote sensing data and measured flux data as training samples (Dong, 2021). Examples include artificial neural networks (ANNs), support vector machines (SVMs), random forests (RFs), and convolutional neural networks (CNNs). A number of studies have proven the excellent performance of machine learning models in simulating vegetation GPP and its time series. For example, Yang et al. (2007) trained an SVM to predict vegetation GPP using explanatory remote sensing variables, such as land surface temperature, the enhanced vegetation index (EVI), land cover, and ground-measured climate variables. A new two-step approach in which an existing emergent constraint on CO_2 fertilization was applied in combination with a supervised machine learning model to constrain uncertainties in multimodel predictions of GPP was proposed (Manuel et al., 2020). Wu et al. (2019) developed a global forest GPP estimation model by using a CNN. The simulation results were verified to be highly consistent with the values observed at flux stations. An ANN was used to estimate the global-scale GPP (142 ± 7.7 Pg C a^{-1}), and the result was not extensively different from that estimated by the Vegetation Photosynthesis Model (VPM) (Zhang et al., 2017), indicating that the machine learning method could effectively capture the uncertainties associated with GPP changes (Joiner and Yoshida, 2020). However, machine learning methods require a large amount of training data to be input, and the simulation results are difficult to interpret these methods display strong regional applicability and relatively poor universality (Yuan et al., 2014a). In addition, most existing machine learning methods are not sufficiently deep; notably, the data-mining process is too shallow to analyse potential data trends in detail. Thus, it is difficult to explain the complex relationships between climate change processes and ecosystems with traditional machine learning methods (Wu et al., 2019). Zhang et al. (2021) developed a machine learning-based scheme to simulate LAI and GPP time series solely based on meteorological variables. The results demonstrated that the machine learning models performed well in simulating the time series of both LAI and GPP. Visibly, once developed and trained, the machine learning models provide fast computing capabilities, and can be conveniently applied to studies at the continental or global scale. However, it is nearly impossible to interpret the processes in

TABLE 1 LUE model structures.

Model	Model structure	Limiting factor calculation method	Temporal resolution	Spatial resolution	Vegetation	References	Related research (China)
GLO-PEM	$GPP = FPAR \times PAR \times \varepsilon_{max} \times f(T_a) \times f(SHD) \times f(SM)$	$f(T_a) = \frac{[(T-T_{min})(T-T_{max})]}{[(T-T_{min})(T-T_{max})-(T-T_{opt})^2]}$	Seasonal	8 km	*PFTs*	Prince Stephen and Goward (1995)	1981-2000
		$f(SM) = 1 - exp(0.081\ (SM - 83.3))$					Total GPP: 5.96 Pg C/a
		$f(SHD) = 1 - 0.05SHD\ (0 < SHD \leq 15)$					Spatial resolution: 8 km Wang et al. (2009)
		$or\ 0.25\ (SHD > 15)$					
		$SHD = SSH - SH$					
EC-LUE	V1: $GPP = FPAR \times PAR \times \varepsilon_{max} \times \min(f(T_a), f(EF))$;	$f(T_a) = \frac{[(T-T_{min})(T-T_{max})]}{[(T-T_{min})(T-T_{max})-(T-T_{opt})^2]}$	Daily	Site scale	forest	Yuan et al. (2006), Yuan et al. (2019)	2000-2009
	V2: $GPP = FPAR \times PAR \times \varepsilon_{max} \times \min(f(T_a), f(EF))$;	V1: $f(EF) = \frac{1}{\beta+1}$;			grass		Total GPP: 6.04 Pg C/a
	V3: $GPP = FPAR \times PAR \times \varepsilon_{max} \times f(CO_2) \times \min(f(T_a), f(VPD))$;	V2: $f(EF) = \frac{LE}{R_n}$;					Spatial resolution: 10 km Li et al. (2013)
		V3: $f(CO_2) = (C_i - \theta)/(C_i + 2\theta), C_i = C_a \times \chi$; $f(VPD) = VPD_0/(VPD + VPD_0)$					
MOD17	$GPP = FPAR \times PAR \times \varepsilon_{max} \times f(TMIN) \times f(VPD)$	$f(TMIN) = 1\ (TMIN > TMIN_{max})$, or $(TMIN - TMIN_{min})/(TMIN_{max} - TMIN_{min})\ (TMIN_{min} \leq TMIN \leq TMIN_{max})$, or $0\ (TMIN < TMIN_{min})$; $f(VPD) = 0\ (VPD > VPD_{max})$, or $(VPD_{max} - VPD)/(VPD_{max} - VPD_{min})\ (VPD_{min} \leq VPD \leq VPD_{max})$, or $1\ (VPD < VPD_{min}$	8-day	1 km	*PFTs*	Justice et al. (2002)	2001-2010
							Total GPP: 5.47 Pg C/a
							Spatial resolution: 0.5° He et al. (2007)
VPM	$GPP = FPAR \times PAR \times \varepsilon_{max} \times f(T_a) \times f(LSWI) \times f(P)$	$f(T_a) = \frac{[(T-T_{min})(T-T_{max})]}{[(T-T_{min})(T-T_{max})-(T-T_{opt})^2]}$	Hourly	1 km	*PFTs*	Pathmathevan et al. (2008), Schaefer et al. (2012)	2006-2008
		$f(LSWI) = (1 + LSWI)/(1 + LSWI_{max})$					Total GPP: 5.0 Pg C/a
							Spatial resolution: 10 km Chen, (2014)
DTEC	$GPP = (\varepsilon_{msu} \times APAR_{su} + \varepsilon_{msh} \times APAR_{sh}) \times f(T_a) \times f(W)$	$f(T_a) = \frac{[(T-T_{min})(T-T_{max})]}{[(T-T_{min})(T-T_{max})-(T-T_{opt})^2]}$	Monthly	0.05°	*PFTs*	He et al. (2013)	2007-2010
		$f(W) = E/E_p$					Total GPP
							7.17 Pg C/a
							Spatial resolution: 0.0727° Zhang et al. (2021a)

(Continued on following page)

10.3389/fenvs.2023.1093095

TABLE 1 (*Continued*) LUE model structures.

Model	Model structure	Limiting factor calculation method	Temporal resolution	Spatial resolution	Vegetation	References	Related research (China)
TL-LUE	$GPP = (\varepsilon_{msu} \times APAR_{su} + \varepsilon_{msh} \times APAR_{sh}) \times f(VPD) \times f(T_a)$	$f(T_a) = \frac{[(T-T_{min})(T-T_{max})]}{[(T-T_{min})(T-T_{max})-(T-T_{opt})^2]}$	Daily	0.05°	*PFTs*	He et al. (2013)	2006-2008
		$f(VPD) = 0\ (VPD > VPD_{max})$, or $(VPD_{max} - VPD)/(VPD_{max} - VPD_{min})\ (VPD_{min} \leq VPD \leq VPD_{max})$, or $1\ (VPD < VPD_{min}$					Total GPP: 7.063 Pg C/a
							Spatial resolution: 500 m Liang and Zhou (2019)

Note: $f(T_a)$ is the air temperature constraint reflecting the temperature limitation of photosynthesis, SHD, is specific humidity deficit (g kg^{-1}), SM, is soil moisture; SSH, is the saturated specific humidity at the air temperature; SH, is the specific humidity of the air, f (VPD) is the VPD, constraint reflecting the stomatal response to the atmospheric water saturation deficit. f (TMIN) the minimum temperature factor; LSWI, is the Land Surface Water Index; $LSWI_{max}$, is the maximum LSWI, during the growing season for each pixel, f (CO_2) is atmospheric CO_2 concentration factor. f (EF) is evaporative fraction factor, C_a is the atmospheric CO_2 concentration, C_i is the CO_2 concentration in the intercellular air spaces of the leaf (ppm), LE, is latent heat, R_n is net radiation; $APAR_{sh}$, is the PAR absorbed by the shaded leaves; $APAR_{su}$, is the PAR absorbed by the sunlit leaves, β is Bowen ration, defined as the ratio of energy available for sensible heating (H, W m^{-2}) to energy available for latent heating (LE, W m^{-2}), χ is the ratio of leaf internal to ambient CO_2, ε_{msh} is the maximum LUE, of shaded leaves, ε_{msu} is the maximum LUE, of sunlit leaves, θ is the CO_2 compensation point in the absence of dark respiration (ppm) and PFT_S, represents the different functional types of vegetation.

the models and gain knowledge of the physiological mechanisms of vegetation processes.

2.2.4 Light use efficiency (LUE) models

In 1972, Monteith first proposed an LUE model based on the principle of light use efficiency. The main idea of this model involves estimating GPP according to the LUE and absorbed photosynthetically active radiation (APAR) of vegetation. LUE models not only consider the relationships among GPP, LUE and environmental factors but also consider the physiological and ecological processes involved in vegetation photosynthesis. These methods have a scientific physiological and ecological basis. At the same time, they characterize a simplified model structure and have greatly improved simulation abilities and application scopes. The model algorithm can be expressed by Eq. 2-2 below:

$$GPP = APAR \times LUE = PAR \times FPAR \times LUE \qquad (2-2)$$

where LUE represents the light use efficiency of vegetation, APAR represents the photosynthetically effective radiation absorbed by the vegetation canopy, FPAR represents the proportion of photosynthetically effective radiation absorbed by the vegetation canopy, and PAR represents the incident photosynthetically effective radiation. In the process of model parameterization, PAR can be directly obtained from meteorological data. The acquisition methods of FPAR include: 1) empirical models based on reflectance vegetation indices and 2) physical estimation models based on radiative transfer theory (Hall et al., 1995). With the wide application of various moderate and high-resolution remote sensing data products, LUE models based on remote sensing data have gradually become the mainstream methods for estimating GPP. The representative models include the Carnegie-Ames-Stanford Approach (CASA) model (Potter et al., 1993), Vegetation Photosynthesis Model (VPM) (Xiao et al., 2004), Eddy Covariance-LUE (EC-LUE) model (Yuan et al., 2006) and MODIS GPP standard product (MOD17) (Heinsch et al., 2006). See Table 1 for the algorithms of these LUE models. Different LUE models adopt different remote sensing parameters, are applicable to different research areas and research purposes, and consider different impact factors.

The maximum light use efficiency (LUE_{max}) of vegetation refers to the utilization rate of photosynthetically effective radiation by vegetation under ideal conditions. This term is a physiological attribute of plants, and its value is directly related to the type of vegetation (Raymond, 1994; Goetz and Prince, 1998). As an important input parameter of the LUE model, LUE_{max} was assumed to be a fixed value for each vegetation type, as these values are generally constant (Heinsch et al., 2006). However, in reality, LUE_{max} values change with variations in vegetation types, time, space, and the vertical structures of vegetation (Xie et al., 2020). As the most important parameter in the LUE model, the LUE_{max} assumption is an important reason for the low accuracies of vegetation productivity model outputs (Yuan et al., 2014a). Potter *et al.* found that the LUE_{max} of global vegetation was 0.389 g C · MJ^{-1} (Potter et al., 1993). Without the limitations associated with climate conditions or other factors, Hunt *et al.* believed that the upper LUE limit was 3.5 g C · MJ^{-1} (Raymond, 1994), while some scholars' research results denote that the LUEs of some herbs and other vegetation can range between 0.09 and 2.16 g C · MJ^{-1} (Ruimy et al.,

TABLE 2 Influencing factors of LUE.

	Influencing factor	Effect of influencing factor on LUE
Vegetation composition and ecophysiological structure factors	Vegetation type	Different vegetation types have different LUEs
	Surface coverage	The higher the species richness is, the higher the LUE vertical utilization is
	Age of the trees	Generally, the LUEs of middle-aged and mature forests are higher than those of young forests
	Canopy structure	The canopy structure affects the absorption of direct and scattered radiation, but the relationship between the two is not clear and needs further study
	Species richness	In ecological areas with mixed vegetation types, selecting a single LUE value introduces large errors
	Tree height	Dwarf trees have higher LUEs because they are not light-saturated and can receive more scattered radiation
	Stomatal conductance	The stomatal conductance and closing speed directly affect the PAR utilization efficiency through the photosynthesis processes and subsequently affect the vegetation LUE
Environmental factors	Moisture	Water is a key factor affecting LUE. Drought and artificial irrigation both affect LUE, but the details need to be explored
	Radiation	A certain radiation range increases LUE, but too much radiation triggers the photoprotection mechanism and inhibits LUE
	Temperature	LUE increases in areas with sufficient water but shows a weak negative correlation in areas experiencing drought
	Carbon dioxide concentration	An increase in the carbon dioxide concentration causes the LUE to increase to some extent
	Scattered radiation	Scattered radiation with a relatively strong penetration ability significantly increases photosynthesis in leaves; the effects are more obvious on indirect canopy than on direct canopies

Note: This table was adapted from (Gao et al., 2021).

1994; McCrady and Jokela, 1998). The comprehensive influence of the geographical distributions of vegetation and climate zones also causes LUE_{max} to show spatial heterogeneity (Zhao et al., 2007). The influences of these different factors on LUE are shown in Table 2. LUE_{max} changes dynamically with the functional type, phenology and environmental stress of the local vegetation. Therefore, the determination and selection of the LUE_{max} value pose very difficult challenges (Zhao et al., 2004; Heinsch et al., 2006). To date, research reflects great differences in the methods used to determine LUE_{max} (Peng et al., 2000). Determining how to reasonably select this value for ecosystems composed of multiple vegetation types is a key and difficult task.

Although LUE models are all constructed on the same theoretical basis, different model stucture parameterization schemes can result in marked discrepancies in GPP estimates. On the one hand, researchers have adopted different LUE calculation methods according to different research purposes, making it difficult to directly compare the research results. On the other hand, the research has shown that the model parameters are simplified and that the LUE_{max} term is set to a fixed value. For example, the MODIS-derived GPP is underestimated to a certain extent, especially in farmland areas, due to the LUE_{max} parameters being unable to distinguish C3 and C4 plants in the model algorithm (Wang et al., 2013; Zhang et al., 2016a). Therefore, Yan et al. (2015) proposed the terrestrial ecosystem carbon (TEC) model to distinguish the LUE of C3 and C4 plants. As plant canopies have higher LUE rates for scattered radiation than for direct radiation, He et al. (2013) proposed a TL-LUE model that stratifies the canopy into sunlit and shaded leaf areas and uses different LUE_{max} and APAR values for them. Yan et al. (2017) further proposed an improved TL light use efficiency model that considered the effects of direct radiation, scattered radiation and C3 and C4 plant differences, thus improving the reliability of the simulation results. Yuan et al. (2019) considered the impact of elevated atmospheric CO_2 concentrations on vegetation growth, coupled the impact of atmospheric CO_2 concentrations on GPP to the EC-LUE model, and enhanced the ability of this remote sensing data-driven LUE model to simulate long-term changes in GPP. Interestingly, Mizunuma *et al.* collected images of a deciduous forest from the top of a flux tower using two different camera systems. At this deciduous woodland site, there was only a moderate relationship between the NDVI from MODIS and the actual GPP over 2 years. However, the LUE model based on vegetation colour indices calculated from digital camera images yielded results with a better correlation with GPP. In particular, the hue parameter was an excellent predictor of GPP over 2 years (Toshie et al., 2013).

In addition to improving and optimizing model algorithms, scholars have also carried out model comparison research based on observed flux data, thus revealing the shortcomings of remote sensing GPP inversion algorithms and the leading influencing factors. The spatiotemporal differences of GPP in China simulated by the MODIS, Breathing Earth System Simulator (BESS) and VPM models were compared. The results showed that the three models could effectively reflect the spatial change pattern of GPP, but great differences were found in the interannual variation of the different models (Chen et al., 2019a). Lin et al. (2018) compared and verified the simulation accuracy of a solar energy utilization model in deciduous coniferous forests, mixed forests, grasslands, farmlands, shrublands, and evergreen broad-leaved forest

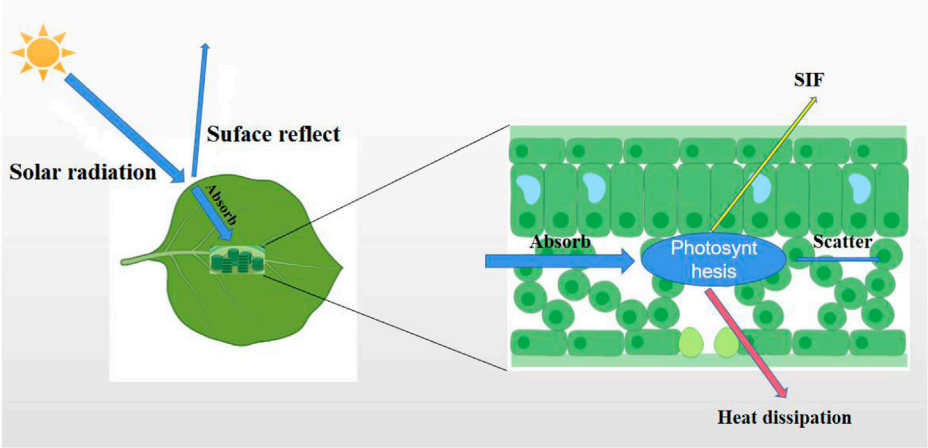

FIGURE 3
The combined process between photosynthesis and SIF.

TABLE 3 Satellite-based sensors used to obtain SIF retrievals currently in orbit.

Platform	Sciamachy	GOSAT	GOME-2	OCO-2	TanSat	TROPOMI
Band (nm)	650–790	755–775	650–790	757–775	758–778	675–775
Spatial Continuity (nm)	0.48	0.025	0.5	0.042	0.044	0.38
Spatial continuity	Continuous	Discrete points	Continuous	Narrow strip	Narrow strip	Continuous
Start-stop time	2003.01-2012.07	2009.12- now	2007.01- now	2014.07- now	2016.12- now	2017.10- now
Transit time	9:30	13:30	9:30	13:30	13:30	13:30
Resolution (km^2)	30 × 240	Diameter 10.5	40 × 80 (2013 and after: 40 × 40)	1.29 × 2.25	1.0 × 2.0	7 × 3
Signal - noise ratio	2800	300	2000	500	360	2660
Revisit period	Approximately 3 days	3 days	Approximately 2 days	16 days	16 days	Approximately 1 day

ecosystems and found that the R^2 values derived between the VPM, EC-LUE and MODIS models were between 0.11 and 0.78, and the root-mean-square errors (RMSE) were between 1.37 and 4.65. Among the analysed ecosystems, the simulation accuracies of every LUE model applied to evergreen broad-leaved forests were low. According to the above findings, although LUE models are relatively mature, uncertainties exist in the accuracy of the estimation results obtained from these models in different regions and for different vegetation types. Therefore, the selection of an appropriate model has a great impact on the GPP estimation results, but the comprehensive estimation ability shown by LUE models is commendable, and these methods can still be considered reliable for estimating the GPP of regional and global terrestrial ecosystems in the future.

2.3 GPP estimations based on sun-induced chlorophyll fluorescence (SIF)

Sun-induced chlorophyll fluorescence (SIF) is a red and near-infrared photon signal based on the absorption of natural light by green plants. This signal can directly reflect dynamic changes in plant photosynthesis. SIF is very sensitive to changes in photosynthesis and is significantly correlated with GPP at the leaf scale (Meroni et al., 2008), plant scale (Damm et al., 2015), canopy scale (Zarco-Tejada et al., 2013) and ecosystem scale (Guanter et al., 2012; Porcar-Castell et al., 2014). Therefore, the use of SIF instead of other vegetation indices has important application prospects with regard to improving GPP estimation accuracies. Some scholars also believe that although there is a strong linear relationship between SIF and GPP, large differences exist in the linear slope of this relationship among different vegetation types (Zhang et al., 2016b). Liu et al. (2022) compared remotely sensed SIF retrievals and satellite-driven GPP products with tower-based GPP measurements in two subtropical forests and reconfirmed the good performance of SIF-based GPP estimation in a multi-year evaluation, with strong linear SIF-GPP relationships observed across two subtropical forest ecosystems. Although there are some uncertainties associated with estimating GPP using SIF inversion techniques, this method still has great potential and developmental prospects.

TABLE 4 Comparison of reconstructed SIF datasets.

Reconstructed dataset name	Variable	Predictor variable	Machine learning method	Spatial resolution	Temporal resolution	References
CSIF	MCD43C4 (first four bands)	OCO-2	Feedforward neural network	0.05	4 days	Zhang et al. (2018a)
		SIF				
RSIF	Aqua-MODIS (four bands)	GOME-2	Feedforward neural network	500 m	—	Gentine and Alemohammad (2018)
		SIF				
$\overline{SIF}_{oco2\_005}$	MCD43C4 (seven bands)	OCO-2	Feedforward neural network	0.05	16 days	Yu et al. (2016)
		SIF				
GOSIF	Landcover	OCO-2	Cubist regression tree	0.05	8 days	Li and Xiao. (2019)
	EVI, VPD, PAR and temperature	SIF				
$\overline{SIF}_{GOME2\_005}$	MCD43C4 (seven bands)	SCIAMA	Random forests and neural networks	0.05	Monthly	Wen et al. (2020)
$\overline{SIF}_{SCIA\_005}$		CHY SIF				
$\overline{SIF}_{005}$		GOME-2				
		SIF				

2.3.1 Development of SIF retrieval methods

SIF is a spectral signal emitted by a photosynthetic centre when green plants absorb solar energy for photosynthesis under natural light conditions. SIF has two peaks corresponding to red light (685 nm) and near-infrared light (740 nm) (Zhang et al., 2019). Moreover, SIF signals are only from the fluorescent emission of vegetation based chlorophyll (shown in Figure 3), which is less affected by the background of cloud and soil conditions than is a vegetation index (Damm et al., 2015; Norton et al., 2018). Therefore, SIF is regarded as an ideal tool for exploring co-occurring vegetation activities and has great application potential for plant growth monitoring (Pradeep et al., 2016). In 2011, National Aeronautics and Space Administration (NASA) scientists first used the Japanese Greenhouse Gases Observing Satellite (GOSAT) to realize the remote sensing inversion of SIF at the global scale (Frankenberg et al., 2011). This work has introduced new innovations and research methods to large-scale vegetation GPP research (Porcar-Castell et al., 2014). The satellite sensors that can currently provide SIF inversion data are shown in Table 3.

Among the spectral signals reflected from the ground surface, chlorophyll fluorescence accounts for approximately 1%–5% of the reflected radiant energy in the near-infrared region. Therefore, it is difficult to directly retrieve chlorophyll fluorescence information from remote sensing data. SIF extraction methods mostly involve calculations based on the Fraunhofer Line Discrimination (FLD) algorithm proposed by Plascyk (Plascyk, 1975). The basic principles are expressed as follows:

$$L(\lambda) = \frac{r(\lambda) \cdot E(\lambda)}{\pi + F(\lambda)} \quad (2-3)$$

$$F_s = \frac{E(\lambda_{out}) \cdot L(\lambda_{in}) - L(\lambda_{out}) \cdot E(\lambda_{in})}{E(\lambda_{out}) - E(\lambda_{in})} \quad (2-4)$$

where λ is the wavelength, $r(\lambda)$ is the true emissivity of vegetation without considering fluorescence, $E(\lambda)$ is the irradiance of the sun incident on the vegetation, $F(\lambda)$ is the chlorophyll fluorescence value induced by sunlight, F_s is the chlorophyll fluorescence value, $E(\lambda_{in})$ and $E(\lambda_{out})$ refer to the incident solar irradiance in the Fraunhofer in-line band and out-of-line band, respectively, and $L(\lambda_{in})$ and $L(\lambda_{out})$ are the apparent radiance in the Fraunhofer in-line band and out-of-line band, respectively.

Although the standard FLD algorithm based on the atmospheric radiative transfer mechanism is simple to operate, the reflectivity and fluorescence values of two adjacent bands are not exactly the same, and this feature affects the accuracy of the fluorescence estimation results. Therefore, a series of improved algorithms have been developed, including the three-band FLD (3FLD) (VanToai et al., 2004) and corrected FLD (cFLD) algorithms (GomezChova et al., 2006) based on multispectral data and the improved FLD (iFLD) (Alonso et al., 2008), extended FLD (eFLD) and spectral fitting method (SFM) algorithms based on hyperspectral data (Meroni and Colombo, 2006). However, when verifying the accuracy of SIF-GPP estimation results, the satellite-derived SIF signal and the GPP value estimated from vorticity-related stations face the problem of spatial inconsistency. Some scholars have conducted relevant research on methods for downscaling and reconstructing SIF data in attempts to overcome the impacts of the different resolutions, physiological characteristics, meteorological conditions and other aspects affecting these data sources. Table 4 shows the available reconstructed SIF datasets. These reconstructed SIF data can effectively reduce the cross-scale mismatch problem and are consistent with both airborne and ground-measured SIF results.

2.3.2 GPP estimation methods based on SIF

At present, research on GPP inversion estimates based on SIF inversions has mostly focused on verifying the correlations between SIF data derived from different sensors and the GPP characterizing different vegetation types. This past research has confirmed the great potential of SIF inversions in estimating GPP. Frankenberg *et al.* and

Guanter et al. observed a high correlation between the SIF values extracted from GOSAT and the GPP values estimated with data-driven methods (Frankenberg et al., 2011; Guanter et al., 2012). Luis *et al.* and Joiner et al. used Global Ozone Monitoring Experiment-2 (GOME-2) SIF data estimations to show that there is good consistency between SIF estimations and the seasonal GPP cycle as measured with flux towers. In addition, the authors reported that the sensitivity of SIF to crop photosynthesis is also higher than those of other existing remotely sensed parameters and models (Joiner et al., 2014; Guanter et al., 2014). Other studies have also verified the effectiveness of estimating GPP from SIF data derived from satellite sensors such as the Orbiting Carbon Observatory-2 (OCO-2) (Sun et al., 2018; Xing et al., 2018), TanSat (Du et al., 2018), and the Tropospheric Monitoring Instrument (TROPOMI) (Damm et al., 2015) through comparisons, indicating that SIF data have great potential for retrieving and estimating GPP.

At present, the high correlation between SIF and GPP is directly used to establish linear regression models between these variables. LUE models based on remote sensing data can be defined as follows:

$$GPP(t) = PAR(t) \times FPAR \times LUE_{p(t)} \quad (2-5)$$

$$SIF(t,\lambda) = PAR(t) \times FPAR \times LUE_f(t,\lambda) \times f_{esc}(\lambda) \quad (2-6)$$

where GPP(t) is the GPP at time t of the day, $LUE_{p(t)}$ is the PAR efficiency at time t, $PAR(t)$ is the photosynthetically effective radiation reaching the canopy at time t, FPAR is the proportion of photosynthetically effective radiation absorbed by the canopy, λ is the wavelength of SIF, $LUE_f(t,\lambda)$ is the fluorescence quantum efficiency, and $f_{esc}(\lambda)$is the probability that the fluorescence emitted by all leaves will escape from the canopy (Joiner et al., 2014). The relationship between *GPP(t) and SIF(t)* can be obtained by combining Eq. (2-2) and Eq. (2-6).

$$GPP(t) = SIF(t,\lambda) \times \frac{1}{f_{esc}(\lambda)} \times \frac{LUE_{p(t)}}{LUE_f(t,\lambda)} \quad (2-7)$$

Near-infrared fluorescence is rarely reabsorbed by leaves or in the canopy, and the canopy structure changes little when a satellite repeatedly covers the same vegetation area within a certain period of time. For the same vegetation type, $f_{esc}(\lambda)$ can be regarded as a constant, especially for grasslands and cultivated lands. Thus, it is assumed that $1/fesc(\lambda) = 1$. Many studies have proven that under the conditions of satellite measurements, $LUEp(t)$ and $LUE_f(t,\lambda)$ tend to change together (Zarco-Tejada et al., 2013; Alexander et al., 2010), and this change can be considered a constant. Therefore, it can be concluded that GPP and SIF are linear.

Based on satellite-derived SIF remote sensing data, a number of studies have estimated GPP at regional and global scales and have achieved good results. Frankenberg et al. (2011) extracted SIF information from GOSAT data using a physical model for the first time and established the relationship between SIF and GPP. The results of their work show that there is a good linear relationship between SIF and GPP on the global scale. Luis *et al.* compared the relationships among GPP, GOME-2 SIF and the MODIS plant index recorded at farmland vorticity flux stations in the United States and found that the relationship between SIF and crop GPP was better than that between the normalized difference vegetation index (NDVI) and crop GPP, the latter relationship exhibited saturation (Guanter et al., 2014). He et al. (2017) corrected the viewing angle of GOME-2 SIF data and calculated the hot spot direction weights (SIF_h) and a weighted sum of SIF (SIF_t) leaves to represent the canopy conditions. The authors concluded that compared to the original SIF observations, the data distinguishing SIF_h and SIF_t had a better correlation with GPP. The authors noted that the SIF760 signal can track the daily dynamics of plant photosynthesis. GPP and SIF760 also showed significant linear correlations every half hour in the canopy of C3 crops (winter wheat) and C4 crops (summer maize), thus further confirming the ability of SIF remote sensing signals to directly estimate GPP (Guan, 2017).

Although global SIF inversion studies have achieved fruitful results, the linear relationship between satellite-derived SIF remote sensing signals and GPP derived based on spatiotemporal merging methods exhibits great differences among different vegetation types due to the strong spatial heterogeneities of ecosystems at spatial scales above 5–10 km (Guanter et al., 2014). Moreover, some scholars have pointed out that the correlation between GPP and SIF at the canopy scale is not a simple linear correlation and that it is more appropriate to use a hyperbolic model to represent this relation (Porcar-Castell et al., 2014; Damm et al., 2015). In addition, the correlation mechanism by which GPP could be estimated using SIF is still unclear. At the same time, the correlation between SIF and GPP is also affected by environmental stressors, canopy structure, local plant functional types and other factors. It is thus necessary to establish a more complete and systematic SIF-GPP research system by combining more accurate observation experiments and improved model algorithms. In summary, research regarding SIF remote sensing inversions and GPP estimations still faces challenges such as low observation accuracies, scale integration issues and model algorithm shortcomings. Moreover, as an effective proxy for terrestrial GPP, SIF reveals a greening trend across most of the world's karst areas. especially for global re-constructed SIF products. Compared with the MODIS GPP product, the SIF observations indirectly confirmed the superior performance of the VPM GPP results (Chen et al., 2019b). This can be ascribed to an improved light use efficiency parameter with the separate treatment for C3/C4 photosynthesis pathways in the VPM model (Tang et al., 2022). This indicates that satellite-based SIF retrievals will have multiple spatial-scale and in broader and more in-depth applications of GPP estimtion.

2.4 GPP estimation methods based on the near-infrared reflectance of vegetation (NIR_v)

Recently, emerging improvements in the direct proxies of GPP, including SIF and NIR_v, have provideed alternative approaches to estimate regional/global GPP(Guanter et al., 2014; Badgley et al., 2017). These indices provide the information on vegetation physiological and biochemical functions (Porcar-Castell et al., 2014; Wang et al., 2019). However, generally limited by satellite-based SIF coarse resolution, short duration (only starting from 1995), and sensor degradation impacts (Zhang et al., 2018b), it can hardly be used to monitor the long-term trends in estimating GPP. The recently proposed NIR_v, is defined as the product of NDVI and near-infrared (NIR) reflectance of vegetation. NIR_v has a robust

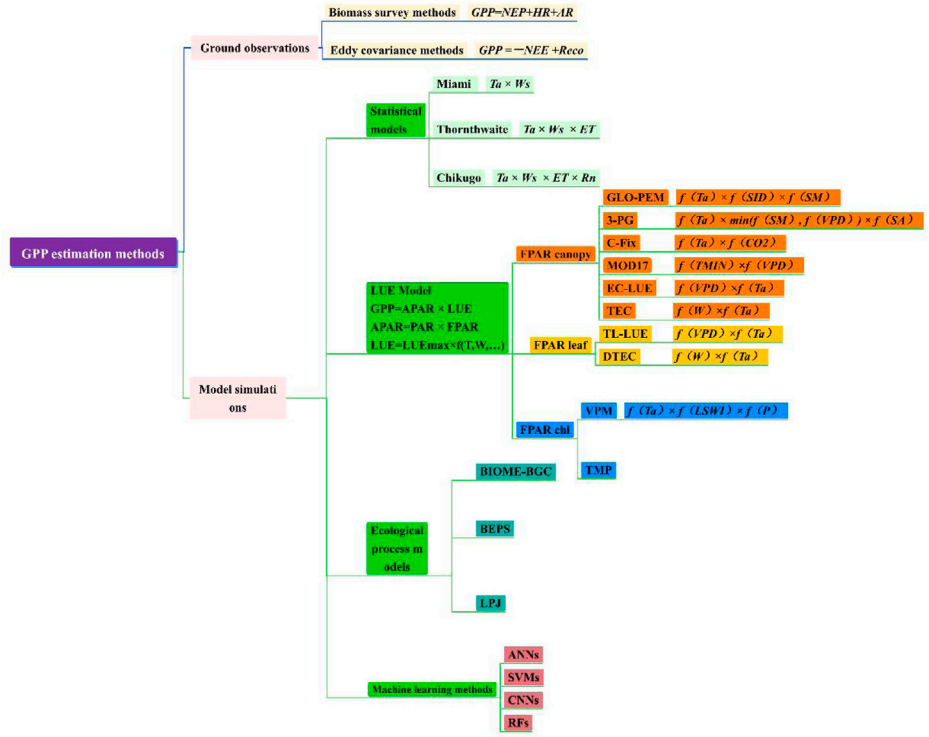

FIGURE 4
Summary of estimation methods of GPP.

physical interpretation, as it relates directly to the number of NIR photons reflected by plants (Badgley et al., 2017). As a result, NIR_v minimizes both the effects of soil contamination and variable viewing geometry on satellite-derived spectra. Compared to NDVI and *f*PAR, NIR_v can better explain GPP flux changes at the monthly and annual scales (56% of monthly changes and 68% of annual changes), and the relationship between NIR_v and GPP is always linear. In addition, the RMSE of GPP simulations performed based on site-based NIR_v was 42% lower than that of the values estimated through BESS model simulations but 57% higher than that of the values estimated using the machine learning product FLUXCOM (Badgley et al., 2017). This indicates that NIR_v can effectively balance the accuracy and complexity of the applied model. Furthermore, the NIR_v approach requires no additional information on meteorological conditions, such as temperature, vapour pressure deficit, or incoming radiation. Residuals in observed GPP relative to NIR_v-derived GPP estimates showed only weak relationships with meteorological variables (Badgley et al., 2017),demonstrating that NIR_v provides a robust basis and new independent method for global estimations of GPP.

Wang et al. (2021) established a robust NIR_v-GPP empirical relationship based on data recorded at hundreds of flux stations and then extended this relationship to the global scale, generating a long-term global GPP product based on Advanced Very High Resolution Radiometer (AVHRR) NIR_v observations. Using this product, the global GPP was estimated to be 128.3 ± 4.0 Pg C yr^{-1}. This result is within the estimation ranges of machine learning methods, LUE models and ecological process models, and the spatial distribution and seasonal pattern are also very similar, indicating that NIR_v can capture long-term GPP trends. According to the absorption and reflection spectra of vegetation, this index can be subdivided into the vegetation near-infrared reflectance ($NIR_{v,\ Ref}$) and vegetation near-infrared emissivity ($NIR_{v,\ Rad}$). However, the relationships between $NIR_{v,\ Ref}$ and GPP on relatively short time scales d) have not been studied, but it is expected that this relationship would be worse than that obtained on the monthly scale because short-term $NIR_{v,Ref}$ changes are much smaller than long-term changes. At this time, the NIR_v of vegetation supplemented by considering incident radiation, $NIR_{v,\ Rad}$, may be the best analogue for obtaining GPP on relatively short time scales (Zeng et al., 2019). Wu et al. (2020) evaluated the GPP performances of corn and soybean with $NIR_{v,\ Rad}$ based on field observations collected across multiple sites. Compared to the other three analysed indicators ($NIR_{v,\ Ref}$, EVI and SIF760), $NIR_{v,\ Rad}$ better explained the changes in GPP. The strong correlations between NIR_v and GPP and between $NIR_{v,\ Rad}$ and GPP prove the robustness of the $NIR_{v,\ Rad}$ indices in estimating GPP across sites, indicating that linear models based on $NIR_{v,\ Rad}$ have great potential for estimating crop GPP at short time scales from high-resolution or long-term satellite remote sensing data. That is, the NIR_v index that considers incident radiation may become a direct substitute for GPP on short time scales.

NIR_v is also highly correlated with SIF and GPP on long-time scales, and these relations have been widely considered by the vegetation remote sensing community. However, NIR_v also has some unsolved problems and shortcomings. For example, as NIR_v is linearly proportional to NIR, how should saturation be

TABLE 5 Summaries of existing GPP research methods.

Research method	Representative model	Advantage	Limitation	Application scope
Biomass survey methods		1) The test method is direct and clear, the research objective is clear and the technical requirement is simple	1) The investigation process is destructive to vegetation	Grasslands, crops, wetlands, forests ecosystems, and other regions that can be set up for quadrat-based data collection
		2) The method by which biomass changes are obtained to estimate NPP and convert NPP to GPP is mature	2) The method involves a large workload, is time consuming and requires a long observation period	
			3) GPP can be calculated only by calculating the proportion of ecological respiration in the study area	
Eddy covariance methods		1) Solid theoretical foundation and high estimation accuracy	1) Flux towers are limited in number and are unevenly distributed	GPP can be obtained for almost all typical ecosystem types, including farmlands, forests, grasslands, wetlands, and lakes. However, this method is limited to areas with vorticity flux stations
		2) The estimation method is reliable and recognized as the standard GPP estimation method	2) The construction of flux towers has high land and underlying surface requirements and high construction costs	
			3) Carbon, water and heat fluxes are not directly available at the regional or global scale	
Statistical models	1) Miami model	1) Simple model structure	1) Lack of a mechanical description	Grasslands, forest ecosystems, etc. However, the climate condition requirements are high, for example, when applying these models to arid and semiarid grasslands, the estimated values are high
	2) Chikugo model	2) The required model parameters are few and easy to obtain	2) The models have strong regional applicability	
	3) Thornthwaite Memorial model		3) It is difficult to predict GPP using these models	
			4) These models have relatively high climatic condition requirements	
Ecological process models	1) BIOME-BGC model	1) Clear description of ecophysiological vegetation processes	1) The model structures are complex	For ecosystem types such as forests, grasslands and farmlands, it is worth noting that the parameterization schemes of these model are adaptable and must be optimized or improved when the models are applied to novel regions
	2) BEPS model	2) These models can be used to perform predictive GPP analyses	2) There are many parameters involved, and some of them are difficult to obtain	
	3) TEM model	3) The GPP estimation results obtained from these models are reliable	3) The regional applicability of these models is strong but is limited by the utilized scale transformation	
	4) CENTURY model			
	5) SIB model			
	6) LPG model			
LUE models	1) CASA model	1) The principle of the models is clear, the calculations are simple, and the models can be applied to obtain large-scale GPP estimations	1) The LUEs of different vegetation types have great spatiotemporal differences	These models are widely used to estimate the GPP of various types of ecosystems. However, it is worth noting that when the vegetation heterogeneity is high in a study area, it is necessary to distinguish the selection of LUEmax values corresponding to different functional plant types
	2) GLO-PEM model	2) Most of the model parameters can be obtained from remote sensing data	2) The chosen data sources and optical transmission process introduce additional uncertainties	
	3) VPM model	3) The simulation accuracy is high, and the high-spatiotemporal-resolution GPP estimates can be obtained		

(Continued on following page)

TABLE 5 (*Continued*) Summaries of existing GPP research methods.

Research method	Representative model	Advantage	Limitation	Application scope
	4) EC-LUE model			
	5) DTEC model			
	6) MODIS product			
Machine learning methods	1) ANNs	1) Feasible methods for effectively solving complex and non-linear problems	1) A large number of training samples need to be input, the availability of which is highly dependent on ground-observed data	These methods are suitable for study areas where large amounts of training data can be obtained, and machine learning methods can be coupled with various models to estimate GPP, including the use of SIF data
	2) SVMs	2) These methods are not affected by the parametric uncertainty of the selected model	2) The simulation results are difficult to explain mechanically	
	3) RFs		1) Climate change and vegetation heterogeneities greatly influence the simulation results	
	4) CNNs			
SIF-GPP	1) Empirical linear models based on the SIF-GPP relation	1) SIF signals come only from vegetation photosynthesis and are less affected by the soil background value and cloud cover conditions	1) SIF signals are very weak, so the spatial and temporal resolutions of ground- and satellite-derived SIF observation data need to be improved	Grasslands, forests, farmlands and other ecosystems, these methods are also used for crop monitoring and phenology-related remote sensing monitoring
	2) Methods based on the SCOPE model	2) The correlation between SIF and GPP is better than those of GPP and other vegetation indices based on greenness	2) The relationship between SIF information collected at different scales and photosynthesis, represents a difficulty in SIF data reconstructions, especially cross-scale simulations	
	3) Methods based on the VPM	3) These methods are ideal for detecting transient photosynthetic vegetation activities		
NIRv-GPP		1) These methods achieve balanced model accuracies and model complexities	1) Some uncertainties exist in the data sources (e.g., cloud contamination)	These methods are most widely applied to farmland ecosystems (especially corn and soybeans)
		2) No additional information on climatic conditions is required	2) There is no physiological explanation for the estimated results	
		3) These methods allow statistically valid error propagations		
		(4)These methods effectively eliminate the impact of the canopy structure		
		5) These calculations can be based on existing high-resolution, widely available satellite imagery		

addressed? In addition, NIR_v uses the same band as NDVI, but it is not clear how the applied assumptions and approximations affect the NIR_v values. These questions need to be explored and answered. At the same time we should also realize that in addition to high accuracy at calibration sites, the approach combines simple calculation, robust error propagation, and the ability to utilize decades of historical remote sensing data. To adapt to the needs of GPP estimation at different spatio-temporal scales. Future refinements of the NIR_v-based approach can come from improved remote sensing inputs and inclusion of additional physiological processes.

3 Comprehensive comparison of GPP research methods

According to the studies and results described above, six conclusions can be obtained: 1) obtaining GPP from flux

observations based on eddy covariance methods is considered to be the most accurate GPP estimation method at present. However, due to the limited number and uneven distribution of flux stations, it is not possible to directly obtain regional/global GPP spatiotemporal patterns through spatial expansion, although the flux data accumulated by EC methods are still indispensable basic data for model simulations and accuracy verifications. 2) Data-driven models lack any description of photosynthetic process mechanisms. 3) Ecological process models have a complete theoretical basis, but the model parameters are numerous and difficult to obtain, and the model structures are relatively complex. 4) Machine learning methods can prevent the uncertainties caused by traditional model parameterization schemes from arising but require the application of a large number of training samples, and the estimation results are difficult to interpret mechanically. 5) The principle of LUE models is clear, and their calculations are simple. Thus, LUE models have become the main tool used to assess regional/global GPP spatial and temporal distributions. However, there are still many deficiencies and defects in these model algorithms and parameterization schemes, and the models need to be further improved and verified. 6) SIF and NIR_v, as direct substitutes of GPP, provide the potential to estimate global GPP, but these correlations are not consistent among different spatiotemporal scales, and the estimation results obtained by these methods lack a clear mechanistic explanation. In summary, the estimation methods of GPP are shown in Figure 4, and the advantages, limitations and application scopes of the various GPP estimation methods reviewed in this paper are summarized comprehensively in Table 5, which provides a model-selection reference for future GPP quantitative research and enables researchers to select accurate estimation models that are suitable for their specific study area.

4 Summary and perspectives

4.1 Summary

A key problem faced in model simulations is the need for comprehensive data with which to parameterize the utilized model and verify the simulation results, especially when performing large-scale estimations. It is necessary to use ground-observed data to improve and optimize the model, and model parameterization errors are one of the main sources of regional/global model estimation errors. First, developing high-precision datasets containing many of the meteorological elements (such as temperature, wind speed, radiation, and precipitation) required in model operation is an important way to improve the simulation accuracies of models. For example, a relatively high spatiotemporal resolution and large observation range can be obtained by using limited meteorological-station-observed data in combination with inverted meteorological satellite-derived data. The massive amounts of data that can be obtained with remote sensing technologies can be effectively screened through comparisons with ground-observed data to obtain the driving data required in regional and even global GPP estimations. Therefore, determining how to extract effective data from long-term, continuous and large-scale remote sensing datasets according to different research purposes in the future has become a key issue faced when attempting to improve the accuracies of model simulations.

Second, we should also be clearly aware that large simulation errors still exist in remote sensing models when assessing some ecosystems with certain vegetation types. For example, in evergreen broad-leaved forests, the accuracies of almost all the models assessed herein are lower than those obtained in other ecosystems (Yuan et al., 2014b), although evergreen broad-leaved forests play a critical role in the global terrestrial carbon cycle (Yuan et al., 2014a). Generalizing the modelling process by considering other ecosystems in global research would introduce large errors, and the reliability of the research results would be controversial. Therefore, it is necessary to improve these model algorithms when simulating specific ecosystem types or typical regions. One important idea involves determining the focused abilities of different models in different ecosystem types according to the accuracy weights of each model algorithm derived for the same ecosystem type and creating multiple model-coupling algorithms to give full play to the advantages of each model and effectively reduce the uncertainty of the simulation results.

In addition, with the development of research needs and technical levels, some indices that perform better than the correlations between vegetation indices and GPP in photosynthesis processes have been found and applied (such as SIF and NIR_v). Of course, it is still very difficult to study the relationship between SIF and GPP on multiple time scales, including at the different growth stages of vegetation, and to study the instantaneous relationship between SIF and GPP. Here, the consideration of the different time scales (minutes to years) provided by the EC method may be an effective way to verify the SIF-GPP relationship on different time scales.

4.2 Perspectives

Generally, accurate driving data, specific algorithm formulas, clear model uncertainties (error ranges) and highly relevant model parameters are important indicators for improving the estimation accuracy of a model and determining the potential application scope of the model. This paper makes the following considerations regarding how to optimize and improve the simulation accuracies of analysed models: 1) the estimation results obtained using different models are quite different. We compared the model structures and evaluated the applicability of each analysed model to effectively reduce the uncertainty introduced by each model itself and improve the overall model simulation accuracy. Therefore, effectively combining the advantages of various models and building a coupled model containing multiple models are important directions for the future development of GPP simulations. For example, the combination of LUE models and machine learning methods may be an important direction for the accurate simulation of terrestrial GPP in the future. 2) Environmental stress factors, including temperature, precipitation, solar radiation, VPD, CO_2 concentration and evapotranspiration, also have important effects on the accuracy of GPP simulations. In model simulation, generally, one or more of these influencing factors are considered, while the

impact of the other factors and their coupling effects on the GPP estimation results are neglected. More factors could be further considered in subsequent research to improve the accuracy of GPP simulations and estimations. 3) The scale transition effect of model simulation applications still represents a popular future research direction. 4) The emerging SIF and NIRv indicators may play an important role in improving the accuracy of LUE models in regional and global GPP simulations. By integrating the SIF indicators into the construction and calibration of LUE models, and considering the evolution characteristics of LUE models, LUE models can potentially be improved in the future.

Author contributions

All authors reviewed and commented on the manuscript. ZL contributed to perform the literature search and data analysis and drafted the article. BZ, HJ, and JZ had the idea for the article, and XF contributed to guiding and revising the manuscript.

Funding

This study was supported by the Science and Technology Research Project of Guizhou Province, China ([2020]1Y073), the National Natural Science Foundation of China (32160290), the Special Research Fund of Natural Science (Special Post) of Guizhou University, China ([2018] 29), the Cultivation Project of Natural Science of Guizhou University, China ([2019]69), and the Opening Fund for Guizhou Province Key Laboratory of Ecological Protection and Restoration of Typical Plateau Wetlands (No. Bikelianhezi Guigongcheng [2021]07), Science and Technology Department of Guizhou Province – the National Government guiding local funds for scientific and technological development ([2022]4022).

Acknowledgments

The authors would like to thank the reviewers and editors for the beneficial and helpful suggestions for this article.

Conflict of interest

The authors declare that the research was conducted in the absence of any commercial or financial relationships that could be construed as a potential conflict of interest.

Publisher's note

References

Alexander, D., Jan, E., Erler, A., Gioli, B., Hamdi, K., Hutjes, R., et al. (2010). Remote sensing of sun-induced fluorescence to improve modeling of diurnal courses of gross primary production (GPP). *Glob. Change Biol.* 16 (1), 171–186. doi:10.1111/j.1365-2486.2009.01908.x

Alonso, L., Gómez-Chova, L., Amoros-Lopez, J., Guanter, L., and Calpe, J. (2008). Improved fraunhofer line discrimination method for vegetation fluorescence quantification. *IEEE Geosci. Remote Sens. Lett.* 5 (4), 620–624. doi:10.1109/lgrs.2008.2001180

Badgley, G., Field, C. B., and Berry, J. A. (2017). Canopy near-infrared reflectance and terrestrial photosynthesis. *Sci. Adv.* 3 (3), e1602244. doi:10.1126/sciadv.1602244

Badgley, G., Anderegg, L. D. L., Berry, J. A., and Field, C. B. (2019). Terrestrial gross primary production: Using NIRV to scale from site to globe. *Glob. Chang. Biol.* 25 (11), 3731–3740. doi:10.1111/gcb.14729

Chapin, F. S., Woodwell, G. M., Randerson, J. T., Rastetter, E. B., Lovett, G. M., Baldocchi, D. D., et al. (2006). Reconciling carbon-cycle concepts, terminology, and methods. *Ecosystems* 9 (7), 1041–1050. doi:10.1007/s10021-005-0105-7

Chen, C., Park, T., Wang, X., Piao, S., Xu, B., Chaturvedi, R. K., et al. (2019b). China and India lead in greening of the world through land-use management. *Nat. Sustain.* 2 (2), 122–129. doi:10.1038/s41893-019-0220-7

Chen, G. (1987). Preliminary study on calculation of primary production of ecosystem in China with application of Miami model model. *J. Nat. Resour.* 3, 270–278. (in chinese)

Chen, J. (2014). *Remote sensing modeling of gross primary productivity in Chinese terrestrial ecosystems*. Beijing: University of Chinese Academy of Sciences.

Chen, J., Yan, H., and Wang, S. (2014). Estimation of gross primary productvity in Chinese terrestrial ecosystems by using VPM model. *Quat. Sci.* 34 (4), 732–742. doi:10.3969/j.issn.1001-7410.2014.04.05

Chen, L. (2017). Comparison of estimated global gross primary productivity and evapotranspiration based on different remote sensing data. Master Thesis. China: China University of Mining and Technology.

Chen, M., Jing, M., Pisek, J., Liu, J., Deng, F., Ishizawa, M., et al. (2012). Effects of foliage clumping on the estimation of global terrestrial gross primary productivity. *Glob. Biogeochem. Cycles* 26 (1). doi:10.1029/2010gb003996

Chen, Y., Gu, H., Wang, M., Gu, Q., Ding, Z., Ma, M., et al. (2019a). Contrasting performance of the remotely-derived GPP products over different climate zones across China. *Remote Sens.* 11 (16), 1855. doi:10.3390/rs11161855

Christian, B., Markus, R., Enrico, T., Ciais, P., Jung, M., Carvalhais, N., et al. (2010). Terrestrial gross carbon dioxide uptake: Global distribution and covariation with climate. *Science* 329 (5993), 834–838. doi:10.1126/science.1184984

Cramer, W., Alberte, B., Ian, W. F., Prentice, I. C., Betts, R. A., Brovkin, V., et al. (2001). Global response of terrestrial ecosystem structure and function to CO2 and climate change: Results from six dynamic global vegetation models. *Glob. Change Biol.* 7 (4), 357–373. doi:10.1046/j.1365-2486.2001.00383.x

Damm, A., Guanter, L., and Paul-Limoges, E. (2015). Far-red sun-induced chlorophyll fluorescence shows ecosystem-specific relationships to gross primary production: An assessment based on observational and modeling approaches. *Remote Sens. Environ.* 166, 91–105. doi:10.1016/j.rse.2015.06.004

Dong, H. (2021). Simulation of vegetation GPP by combining flux observation site data and light energy efficiency model. Master Thesis. Zhejiang: Zhejiang A&F University.

Du, S., Liu, L., Liu, X., Zhang, X., Zhang, X., Bi, Y., et al. (2018). Retrieval of global terrestrial solar-induced chlorophyll fluorescence from TanSat satellite. *Sci. Bull.* 63 (22), 1502–1512. doi:10.1016/j.scib.2018.10.003

Fei, X. (2018). *Carbon exchanges and their responses to climate change in representative forest ecosystems in Yunnan, SW China*. Beijing: University of Chinese Academy of Sciences, 220.

Feng, X., Liu, G., and Chen, S. (2004). Study on process model of net primary productivity of terrestrial ecosystems. *J. Nat. Resour.* 3, 369–378. (in chinese)

Frankenberg, C., Fisher, S., Badgley, G., Saatchi, S. S., Lee, J. E., et al. (2011). New global observations of the terrestrial carbon cycle from GOSAT: Patterns of plant fluorescence with gross primary productivity. *Geophys. Res. Lett.* 38 (17), 48738. doi:10.1029/2011gl048738

Friend Andrew, D., Almut, A., Kiang Nancy, Y., Lomas, M., Ogee, J., Rodenbeck, C., et al. (2007). FLUXNET and modelling the global carbon cycle. *Glob. Change Biol.* 13 (3), 610–633. doi:10.1111/j.1365-2486.2006.01223.x

Gao, D., Wang, S., and Yan, L. (2021). Light use efficiency of vegetation:model and uncertainty. *Acta Ecol. Sin.* 14, 1–11. doi:10.5846/stxb202003210624

Gentine, P., and Alemohammad, S. H. (2018). Reconstructed solar-induced fluorescence: A machine learning vegetation product based on MODIS surface reflectance to reproduce GOME-2 solar-induced fluorescence. *Geophys. Res. Lett.* 45 (7), 3136–3146. doi:10.1002/2017gl076294

Goetz, J., and Prince, D. (1998). Variability in carbon exchange and light utilization among boreal forest stands: Implications for remote sensing of net primary production. *Can. J. For. Res.* 28 (3), 375–389. doi:10.1139/x97-222

GomezChova, L., AlonsoChorda, L., and Amoros, L. J. (2006). Solar induced fluorescence measurements using a field spectroradiometer. *AIP Conf. Proc.* 852 (1), 274. doi:10.1063/1.2349354

Guan, L. (2017). Estimation of gross primary production using sun-induced chlorophyll fluorescence. Master Thesis. Beijing: University of Chinese Academy of Sciences.

Guanter, L., Christian, F., and Anu, D. (2012). Retrieval and global assessment of terrestrial chlorophyll fluorescence from GOSAT space measurements. *Remote Sens. Environ.* 121, 236–251. doi:10.1016/j.rse.2012.02.006

Guanter, L., Zhang, Y., Jung, M., Joiner, J., Voigt, M., Berry, J. A., et al. (2014). Global and time-resolved monitoring of crop photosynthesis with chlorophyll fluorescence. *Proc. Natl. Acad. Sci. U. S. A.* 111 (14), E1327–E1333. doi:10.1073/pnas.1320008111

Hall, G., Thomas, H., and Coops Nicholas, C. (2012). Data assimilation of photosynthetic light-use efficiency using multi-angular satellite data: I. Model formulation. *Remote Sens. Environ.* 121, 273–300. doi:10.1016/j.rse.2012.02.008

Hall, G., Townshend John, R., and Engman Edwin, T. (1995). Status of remote sensing algorithms for estimation of land surface state parameters. *Remote Sens. Environ.* 51 (1), 138–156. doi:10.1016/0034-4257(94)00071-t

He, L., Chen Jing, M., Liu, J., Mo, G., and Joiner, J. (2017). Angular normalization of GOME-2 Sun-induced chlorophyll fluorescence observation as a better proxy of vegetation productivity. *Geophys. Res. Lett.* 44 (11), 5691–5699. doi:10.1002/2017gl073708

He, M., Ju, W., Zhou, Y., Chen, J., He, H., Wang, S., et al. (2013). Development of a two-leaf light use efficiency model for improving the calculation of terrestrial gross primary productivity. *Agric. For. Meteorology* 173, 28–39. doi:10.1016/j.agrformet.2013.01.003

He, Y., Dong, W., Dong, X., and Dan, L. (2007). Terrestrial growth in China and its relationship with climate based on the MODIS data. *Acta Ecol. Sin.* 27 (12), 5086–5092. doi:10.1016/s1872-2032(08)60015-3

Heinsch, F. A., Zhao Maosheng, S. W. R., Kimball, J., Nemani, R., and Davis, K. (2006). Evaluation of remote sensing based terrestrial productivity from MODIS using regional tower eddy flux network observations. *Ieee Trans. Geoscience Remote Sens.* 44 (7), 1908–1925. doi:10.1109/tgrs.2005.853936

Helmut, L. (1975). Modeling the primary productivity of the world, Primary productivity of the biosphere. *Springer*, 237–263. doi:10.1007/978-3-642-80913-2_12

Huang, P. (2019). Estimation of global terrestrial gross primary productivity based on solar-induced chlorophyll fluorescence. Master Thesis. Wuhan: Wuhan University of Technology.

Huang, Z. (2000). Application of a Century model to management effects in the productivity of foresta in Dinghushan. *Acta Phytoecol. Sin.* 2, 175–179.

Joiner, J., and Yoshida, Y. (2020). Satellite-based reflectances capture large fraction of variability in global gross primary production (GPP) at weekly time scales. *Agric. For. Meteorology* 291, 108092. doi:10.1016/j.agrformet.2020.108092

Joiner, J., Yoshida, Y., Vasilkov, A. P., Schaefer, K., and Jung, M. (2014). The seasonal cycle of satellite chlorophyll fluorescence observations and its relationship to vegetation phenology and ecosystem atmosphere carbon exchange. *Remote Sens. Environ.* 152, 375–391. doi:10.1016/j.rse.2014.06.022

Justice, C. O., Townshend, J. R. G., Vermote, E. F., Masuoka, E., Wolfe, R., Saleous, N., et al. (2002). An overview of MODIS Land data processing and product status. *Remote Sens. Environ.* 83 (1), 3–15. doi:10.1016/s0034-4257(02)00084-6

Li, X., Liang, S., Yu, G., Yuan, W., Cheng, X., Xia, J., et al. (2013). Estimation of gross primary production over the terrestrial ecosystems in China. *Ecol. Model.* 261-262, 80–92. doi:10.1016/j.ecolmodel.2013.03.024

Li, X., and Xiao, J. (2019). Mapping photosynthesis solely from solar-induced chlorophyll fluorescence: A global, fine-resolution dataset of gross primary production derived from OCO-2. *Remote Sens.* 11 (21), 2563. doi:10.3390/rs11212563

Liang, S., Rui, B., and Chen, X. (2020). Review of China's land surface quantitative remote sensing development in 2019. *J. Remote Sens.* 24 (06), 618–671. doi:10.11834/jrs.20209476

Liang, S., and Zhou, Y. (2019). Consistency analysis of global GPP products and GPP simulated by two-leaf light use efficiency model. *J. Shaanxi Normal Univ. Nat. Sci. Ed.* 47 (03), 103–114. doi:10.15983/j.cnki.jsnu.2019.03.432

Lim, K., Treitz, P., Wulder, M., St-Onge, B., and Flood, M. (2003). LiDAR remote sensing of forest structure. *Prog. Phys. Geogr.* 27 (1), 88–106. doi:10.1191/0309133303pp360ra

Lin, S., jing, L., and Liu, Q. (2018). Overview on estimation accuracy of gross primary productivity with remote sensing methods. *J. Remote Sens.* 22 (2), 234–254. doi:10.11834/jrs.20186456

Liu, G., Wang, Y., Chen, Y., Tong, X., and Xie, J. (2022). Remotely monitoring vegetation productivity in two contrasting subtropical forest ecosystems using solar-induced chlorophyll fluorescence. *Remote Sens.* 14 (6), 1328. doi:10.3390/rs14061328

Liu, J., Chen, J. M., and Cihlar, J. (1997). A process-based boreal ecosystem productivity simulator using remote sensing inputs. *Remote Sens. Environ.* 62 (2), 158–175. doi:10.1016/s0034-4257(97)00089-8

Ma, J., Yan, X., Dong, W., and Chou, J. (2015). Gross primary production of global forest ecosystems has been overestimated. *Sci. Rep.* 5 (1), 10820. doi:10.1038/srep10820

Manuel, S., Veronika, E., Gustau, C. V., Friedlingstein, P., Gentine, P., and Reichstein, M. (2020). Constraining uncertainty in projected gross primary production with machine learning. *J. Geophys. Res. Biogeosciences* 125 (11), 5619. doi:10.1029/2019jg005619

McCrady, R. L., and Jokela, E. J. (1998). Canopy dynamics, light interception, and radiation use efficiency of selected loblolly pine families. *For. Sci.* 44, 1. doi:10.1093/forestscience/44.1.64

Meroni, M., and Colombo, R. (2006). Leaf level detection of solar induced chlorophyll fluorescence by means of a subnanometer resolution spectroradiometer. *Remote Sens. Environ.* 103 (4), 438–448. doi:10.1016/j.rse.2006.03.016

Meroni, M., Picchi, V., Rossini, M., Cogliati, S., Panigada, C., Nali, C., et al. (2008). Leaf level early assessment of ozone injuries by passive fluorescence and photochemical reflectance index. *Int. J. Remote Sens.* 29 (17-18), 5409–5422. doi:10.1080/01431160802036292

Norton, J., Rayner Peter, J., Koffi Ernest, N., and Scholze, M. (2018). Assimilating solar-induced chlorophyll fluorescence into the terrestrial biosphere model BETHY-SCOPE v1.0: Model description and information content. *Geosci. Model. Dev.* 11 (4), 1517–1536. doi:10.5194/gmd-11-1517-2018

Pathmathevan, M., Wofsy Steven, C., Matross Daniel, M., Xiao, X., Dunn, A. L., Lin, J. C., et al. (2008). A satellite-based biosphere parameterization for net ecosystem CO2 exchange: Vegetation Photosynthesis and Respiration Model (VPRM). *Glob. Biogeochem. Cycles* 22 (2), 2735. doi:10.1029/2006gb002735

Peng, S., Guo, Z., and Wang, B. (2000). Use of GIS and RS to estimate the light utilization efficiency of the vegetation in Guangdong, China. *Acta Ecol. Sin.* (6), 903–909. (in chinese)

Plascyk, A. (1975). The MK II fraunhofer line discriminator (FLD-II) for airborne and orbital remote sensing of solar-stimulated luminescence. *Opt. Eng.* 14 (4), 1842. doi:10.1117/12.7971842

Porcar-Castell, A., Tyystjärvi, E., Atherton, J., van der Tol, C., Flexas, J., Pfundel, E. E., et al. (2014). Linking chlorophyll a fluorescence to photosynthesis for remote sensing applications: Mechanisms and challenges. *J. Exp. Bot.* 65 (15), 4065–4095. doi:10.1093/jxb/eru191

Potter, S., Randerson James, T., Field Christopher, B., Matson, P. A., Vitousek, P. M., Mooney, H. A., et al. (1993). Terrestrial ecosystem production: A process model based on global satellite and surface data. *Glob. Biogeochem. Cycles* 7 (4), 811–841. doi:10.1029/93gb02725

Powell Scott, L., Cohen Warren, B., Healey Sean, P., Kennedy, R. E., Moisen, G. G., Pierce, K. B., et al. (2009). Quantification of live aboveground forest biomass dynamics with landsat time-series and field inventory data: A comparison of empirical modeling approaches. *Remote Sens. Environ.* 114 (5), 1053–1068. doi:10.1016/j.rse.2009.12.018

Pradeep, W., Zhang, Y., Jin, C., and Xiao, X. (2016). Comparison of solar-induced chlorophyll fluorescence, light-use efficiency, and process-based GPP models in maize. *Ecol. Appl. Publ. Ecol. Soc. Am.* 26 (4), 1211–1222. doi:10.1890/15-1434

Prince Stephen, D., and Goward, S. N. (1995). Global primary production: A remote sensing approach. *J. Biogeogr.* 22, 815. doi:10.2307/2845983

Qiu, K. (2015). *Estimating regional vengetation gross primary productivity (GPP),evapotranspiration(ET),water use efficiency(WUE) and their spatial and temporal distribution across China*. Beijing: Beijing Forestry University.

Rahman, M. M., Lamb, D. W., and Stanley, J. N. (2015). The impact of solar illumination angle when using active optical sensing of NDVI to infer fAPAR in a pasture canopy. *Agric. For. Meteorology* 202, 39–43. doi:10.1016/j.agrformet.2014.12.001

Raymond, H. E. (1994). Relationship between woody biomass and PAR conversion efficiency for estimating net primary production from NDVI. *Int. J. Remote Sens.* 15 (8), 1725–1729. doi:10.1080/01431169408954203

Ruimy, A., Saugier, B., and Dedieu, G. (1994). Methodology for the estimation of terrestrial net primary production from remotely sensed data. *J. Geophys. Res. Atmos.* 99 (D3), 5263. doi:10.1029/93jd03221

Running Steven, W. (1993). "Generalization of a forest ecosystem process model for other biomes, Biome-BGC, and an application for global-scale models," in *Scaling processes between leaf and landscape levels. Scaling physiological processes: Leaf to globe* (San Diego: Academic Press), 141–158. doi:10.1016/B978-0-12-233440-5.50014-2

Running Steven, W., and Joseph, C. (1988). A general model of forest ecosystem processes for regional applications I. Hydrologic balance, canopy gas exchange and primary production processes. *Ecol. Model.* 42 (2), 125–154. doi:10.1016/0304-3800(88)90112-3

Schaefer, K., Schwalm, M., Williams, C., Arain, M. A., Barr, A., Chen, J. M., et al. (2012). A model-data comparison of gross primary productivity: Results from the north American carbon program site synthesis. *J. Geophys. Res. Biogeosciences* 117 (G3), 1960. doi:10.1029/2012jg001960

Schimel, D., Ryan, P., Fisher Joshua, B., Asner, G. P., Saatchi, S., Townsend, P., et al. (2015). Observing terrestrial ecosystems and the carbon cycle from space. *Glob. Change Biol.* 21 (5), 1762–1776. doi:10.1111/gcb.12822

Sellers, P. J., Randall, D. A., and Collatz, G. J. (1996). *A revised land surface parameterization for atmospheric GCMS. Part I: Model formulation. American Meteorological Society*. doi:10.1175/1520-0442(1996)009>0676:ARLSPF>2.0.CO;2

Shi, X. (2019). Factors affecting the temperature sensitivity of gross primary productivity in typical forests of China. Master Thesis. Beijing: Beijing Forestry University.

Sinha, S., Jeganathan, C., Sharma, L. K., and Nathawat, M. S. (2015). A review of radar remote sensing for biomass estimation. *Int. J. Environ. Sci. Technol.* 12 (5), 1779–1792. doi:10.1007/s13762-015-0750-0

Sitch, S., Smith, B., Prentice, I. C., Arneth, A., Bondeau, A., Cramer, W., et al. (2003). Evaluation of ecosystem dynamics, plant geography and terrestrial carbon cycling in the LPJ dynamic global vegetation model. *Glob. Change Biol.* 9 (2), 161–185. doi:10.1046/j.1365-2486.2003.00569.x

Sun, Y., Christian, F., and Jung, M. (2018). Overview of solar-induced chlorophyll fluorescence (SIF) from the orbiting carbon observatory-2: Retrieval, cross-mission comparison, and global monitoring for GPP. *Remote Sens. Environ.* 209, 808–823. doi:10.1016/j.rse.2018.02.016

Tang, X., Li, H., Ni, H., Li, X., Xu, X., Ding, Z., et al. (2015). A comprehensive assessment of MODIS-derived GPP for forest ecosystems using the site-level FLUXNET database. *Environ. Earth Sci.* 74 (7), 5907–5918. doi:10.1007/s12665-015-4615-0

Tang, X., Xiao, J., and Ma, M. (2022). Satellite evidence for China's leading role in restoring vegetation productivity over global karst ecosystems. *For. Ecol. Manag.* 507, 120000. doi:10.1016/j.foreco.2021.120000

Tian, H., ChenZhang, C., Sun, G., and Lu, C. (2010). Model estimates of net primary productivity, evapotranspiration, and water use efficiency in the terrestrial ecosystems of the southern United States during 1895-2007. *For. Ecol. Manag.* 259 (7), 1311–1327. doi:10.1016/j.foreco.2009.10.009

Toshie, M., Matthew, W., Eaton Edward, L., Mencuccini, M., I. L. Morison, J., and Grace, J. (2013). The relationship between carbon dioxide uptake and canopy colour from two camera systems in a deciduous forest in southern England. *Funct. Ecol.* 27 (1), 196–207. doi:10.1111/1365-2435.12026

Uchijima, Z., and Seino, H. (1985). Agroclimatic evaluation of net primary productivity of natural vegetations. *J. Agric. Meteorology* 40 (4), 343–352. doi:10.2480/agrmet.40.343

VanToai, T., Major, D., and McDonald, M. (2004). Digital imaging and spectral techniques: Applications to precision agriculture and crop physiology. *American Society of Agronomy, Crop Science Society of America, and Soil Science Society of America*. doi:10.2134/ASASPECPUB66

Wang, K., Wang, H., and Sun, J. (2017). Application and comparison of remote sensing GPP models with multi-site data in China. *Chin. J. Plant Ecol.* 41 (03), 337–347. (in chinese) doi:10.17521/cjpe.2016.0182

Wang, L., Ding, J., and Yonghua, J. (2009). Spatiotem poral pattern of NPP in terrestrial ecosystem of China from 1981 to 2000. *Joumal Jiangsu For. Sci.* and *Technology* 36 (06), 1–5. (in chinese)

Wang, S., Grant, R. F., Verseghy, D. L., and Black, T. (2001). Modelling plant carbon and nitrogen dynamics of a boreal aspen forest in CLASS — The Canadian land surface scheme. *Ecol. Model.* 142 (1), 135–154. doi:10.1016/s0304-3800(01)00284-8

Wang, S., Ju, W., Peñuelas, J., Cescatti, A., Zhou, Y., Fu, Y., et al. (2019). Urban-rural gradients reveal joint control of elevated CO2 and temperature on extended photosynthetic seasons. *Nat. Ecol. Evol.* 3 (7), 1076–1085. doi:10.1038/s41559-019-0931-1

Wang, S., Zhang, Y., Ju, W., Qiu, B., and Zhang, Z. (2021). Tracking the seasonal and inter-annual variations of global gross primary production during last four decades using satellite near-infrared reflectance data. *Sci. Total Environ.* 755 (2), 142569. doi:10.1016/j.scitotenv.2020.142569

Wang, X., Ma, M., Xin, L., Song, Y., Tan, J., Huang, G., et al. (2013). Validation of MODIS-GPP product at 10 flux sites in northern China. *Int. J. Remote Sens.* 34 (2), 587–599. doi:10.1080/01431161.2012.715774

Wen, C., Sun, C., and Liu, T. (2014). Model methods and mechanisms of vegetation NPP estimation. *Anhui Agri.Sci* 20 (08), 30–33+117. doi:10.16377/j.cnki.issn1007-7731.2014.08.019

Wen, J., Köhler, P., Duveiller, G., Parazoo, N., Magney, T., Hooker, G., et al. (2020). A framework for harmonizing multiple satellite instruments to generate a long-term global high spatial-resolution solar-induced chlorophyll fluorescence (SIF). *Remote Sens. Environ.* 239 (C), 111644. doi:10.1016/j.rse.2020.111644

Wickens, G. E., Lieth, H., and Whittaker, R. H. (1977). Primary productivity of the biosphere. *Kew Bull.* 32 (1), 274. doi:10.2307/4117293

Wohlfahrt, G., and Gu, L. (2015). The many meanings of gross photosynthesis and their implication for photosynthesis research from leaf to globe. *Plant, Cell. and Environ.* 38 (12), 2500–2507. doi:10.1111/pce.12569

Wu, G., Guan, K., Jiang, C., Peng, B., Kimm, H., Chen, M., et al. (2020). Radiance-based NIRv as a proxy for GPP of corn and soybean. *Environ. Res. Lett.* 15 (3), 034009. doi:10.1088/1748-9326/ab65cc

Wu, W., Gong, C., Li, X., Guo, H., and Zhang, L. (2019). An online deep convolutional model of gross primary productivity and net ecosystem exchange estimation for global forests. *IEEE J. Sel. Top. Appl. Earth Observations Remote Sens.* 12 (12), 5178–5188. doi:10.1109/jstars.2019.2954556

Xiao, J., Frederic, C., and Gomez, C. (2019). Remote sensing of the terrestrial carbon cycle: A review of advances over 50 years. *Remote Sens. Environ.* 233, 111383. doi:10.1016/j.rse.2019.111383

Xiao, X., Zhang, Q., and Bobby, B. (2004). Modeling gross primary production of temperate deciduous broadleaf forest using satellite images and climate data. *Remote Sens. Environ.* 91 (2), 256–270. doi:10.1016/j.rse.2004.03.010

Xie, X., Li, A., Tan, J., Jin, H., Nan, X., Zhang, Z., et al. (2020). Assessments of gross primary productivity estimations with satellite data-driven models using eddy covariance observation sites over the northern hemisphere. *Agric. For. Meteorology* 280 (C), 107771. doi:10.1016/j.agrformet.2019.107771

Xing, L., Xiao, J., He, B., Altaf Arain, M., Beringer, J., Desai, A. R., et al. (2018). Solar-induced chlorophyll fluorescence is strongly correlated with terrestrial photosynthesis for a wide variety of biomes: First global analysis based on OCO-2 and flux tower observations. *Glob. Change Biol.* 24 (9), 3990–4008. doi:10.1111/gcb.14297

Yan, H., Wang, S. Q., Yu, K., Wang, B., Yu, Q., Bohrer, G., et al. (2017). A novel diffuse fraction-based two-leaf light use efficiency model: An application quantifying photosynthetic seasonality across 20 AmeriFlux flux tower sites. *J. Adv. Model. Earth Syst.* 9 (6), 2317–2332. doi:10.1002/2016ms000886

Yan, H., Wang, S., Oechel, W., Bohrer, G., Meyers, T., Dave, B., et al. (2015). Improved global simulations of gross primary product based on a new definition of water stress factor and a separate treatment of C3 and C4 plants. *Ecol. Model.* 297, 42–59. doi:10.1016/j.ecolmodel.2014.11.002

Yang, F., Kazuhito, I., White, M. A., Hashimoto, H., Michaelis, A. R., Votava, P., et al. (2007). Developing a continental-scale measure of gross primary production by combining MODIS and AmeriFlux data through Support Vector Machine approach. *Remote Sens. Environ.* 110 (1), 109–122. doi:10.1016/j.rse.2007.02.016

Yu, G., Ren, W., Chen, Z., Zhang, L., Wang, Q., Wen, X., et al. (2016). Construction and progress of Chinese terrestrial ecosystem carbon, nitrogen and water fluxes coordinated observation. *J. Geogr. Sci.* 26 (7), 803–826. doi:10.1007/s11442-016-1300-5

Yuan, W., Cai, W., and Liu, D. (2014a). Satellite-based vegetation production models of terrestrial ecosystem: An overview. *Adv. Earth Sci.* 29 (05), 541–550. doi:10.11867/j.issn.1001-8166.2014.05.0541

Yuan, W., Cai, W., Xia, J., Chen, J., Liu, S., Dong, W., et al. (2014b). Global comparison of light use efficiency models for simulating terrestrial vegetation gross primary production based on the LaThuile database. *Agric. For. Meteorology* 192-193, 108–120. doi:10.1016/j.agrformet.2014.03.007

Yuan, W., Liu, S., Zhou, G., Tieszen, L. L., and Baldocchi, D. (2006). Deriving a light use efficiency model from eddy covariance flux data for predicting daily gross primary production across biomes. *Agric. For. Meteorology* 143 (3), 189–207. doi:10.1016/j.agrformet.2006.12.001

Yuan, W., Zheng, Y., Piao, S., Ciais, P., Lombardozzi, D., Wang, Y., et al. (2019). Increased atmospheric vapor pressure deficit reduces global vegetation growth. *Sci. Adv.* 5 (8), eaax1396. doi:10.1126/sciadv.aax1396

Zarco-Tejada, P. J., Morales, A., Testi, L., and Villalobos, F. (2013). Spatio-temporal patterns of chlorophyll fluorescence and physiological and structural indices acquired from hyperspectral imagery as compared with carbon fluxes measured with eddy covariance. *Remote Sens. Environ.* 133, 102–115. doi:10.1016/j.rse.2013.02.003

Zeng, Y., Grayson, B., Benjamin, D., Ryu, Y., Chen, M., and Berry, J. (2019). A practical approach for estimating the escape ratio of near-infrared solar-induced chlorophyll fluorescence. *Remote Sens. Environ.* 232 (C), 111209. doi:10.1016/j.rse.2019.05.028

Zhang, N. (2020). Estimation of gross primary productivity in heihe river basin by remote sensing and analysis of driving factors. Master Thesis. Xian: Xi 'an University of Science and Technology.

Zhang, X., Wang, H., and Yan, H. (2021a). Analysis of spatio-temporal changes of gross primary productivity in China from 2001 to 2018 based 2018 on Romote Sensing. *Acta Ecol. Sin.* 16, 1–12. doi:10.5846/stxb202010302781

Zhang, Y., Joiner, J., Gentine, P., and Zhou, S. (2018a). Reduced solar-induced chlorophyll fluorescence from GOME-2 during Amazon drought caused by dataset artifacts. *Glob. Change Biol.* 24 (6), 2229–2230. doi:10.1111/gcb.14134

Zhang, Y., Liang, S., and Lu, Y. (2019a). A review of regional and global gridded forest biomass datasets. *Remote Sens.* 11 (23), 2744. doi:10.3390/rs11232744

Zhang, Y., Xiao, X., Wu, X., Zhou, S., Zhang, G., Qin, Y., et al. (2017). A global moderate resolution dataset of gross primary production of vegetation for 2000-2016. *Sci. Data* 4 (1), 170165. doi:10.1038/sdata.2017.165

Zhang, Y., Guanter, L., and Berry Joseph, A. (2016b). Model-based analysis of the relationship between sun-induced chlorophyll fluorescence and gross primary production for remote sensing applications. *Remote Sens. Environ.* 187, 145–155. doi:10.1016/j.rse.2016.10.016

Zhang, Y., Joiner, J., Zhou, S., and Gentine, P. (2018b). A global spatially contiguous solar-induced fluorescence (CSIF) dataset using neural networks. *Biogeosciences* 15 (19), 5779–5800. doi:10.5194/bg-15-5779-2018

Zhang, Y., Xiao, X., Cui, J., Dong, J., Zhou, S., Wagle, P., et al. (2016a). Consistency between sun-induced chlorophyll fluorescence and gross primary production of vegetation in North America. *Remote Sens. Environ.* 183, 154–169. doi:10.1016/j.rse.2016.05.015

Zhang, Z., Wang, S., and Qiu, B. (2019b). Retrieval of sun-induced chlorophyll fluorescence and advancements in carbon cycle application. *J. Remote Sens.* 23 (01), 37–52. doi:10.11834/jrs.20197485

Zhang, Z., Xin, Q., and Li, W. (2021b). Machine learning-based modeling of vegetation leaf area index and gross primary productivity across north America and comparison with a process-based model. *J. Adv. Model. Earth Syst.* 13 (10), 2802. doi:10.1029/2021ms002802

Zhao, M., Liu, Y., and Yang, J. (2019). Spatio-temporal patterns of NPP and its relations to climate in China based on HASM. *Ecol. Environ. Sci.* 28 (2), 215–225. doi:10.16258/j.cnki.1674-5906.2019.02.001

Zhao, M., Heinsch Faith AnnNemani Ramakrishna, R., and Running, S. W. (2004). Improvements of the MODIS terrestrial gross and net primary production global data set. *Remote Sens. Environ.* 95 (2), 164–176. doi:10.1016/j.rse.2004.12.011

Zhao, Y., Liu, S., and Junbang, W. (2007). Light use efficiency of vegetation:A review. *Chin. J. Ecol.* 9, 1471–1477.

Zhu, J., Gao, T., and Yu, L. (2021). Functions and applications of multi-tower platform of qingyuan forest ecosystem research station of Chinese Academy of Sciences (Qingyuan Ker Towers). *Proc. Chin. Acad. Sci.* 36 (03), 351–361+371. doi:10.16418/j.issn.1000-3045.20210304002

Zhu, T. (2021). Study on estimation of vegetation gross primary productivity based on CNN deep learning model in China. Master Thesis. Gansu: Northwest Normal University.